inorganics

MDPI

Article

Backbone-Substituted β-Ketoimines and Ketoiminate Clusters: *Transoid* Li_2O_2 Squares and D_2-Symmetric Li_4O_4 Cubanes. Synthesis, Crystallography and DFT Calculations

Twyla Gietz [1] and René T. Boeré [1,2,*]

[1] Department of Chemistry and Biochemistry, University of Lethbridge, Lethbridge, AB T1K3M4, Canada; tweetersrd_22@hotmail.com

[2] The Canadian Centre for Research in Advanced Fluorine Technologies, University of Lethbridge, Lethbridge, AB T1K3M4, Canada

* Correspondence: boere@uleth.ca; Tel.: +1-403-329-2045

Academic Editor: Matthias Westerhausen
Received: 31 March 2017; Accepted: 21 April 2017; Published: 26 April 2017

Abstract: The preparation and crystal structures of four β-ketoimines with bulky aryl nitrogen substituents (2,6-diisopropylphenyl and 2,4,6-trimethylphenyl) and varying degrees of backbone methyl substitution are reported. Backbone substitution "pinches" the chelate ring. Deprotonation with *n*-butyllithium leads to dimeric Li_2O_2 clusters, as primary laddered units, with an open *transoid* geometry as shown by crystal structures of three examples. The coordination sphere of each lithium is completed by one tetrahydrofuran ligand. NMR spectra undertaken in either C_6D_6 or 1:1 C_6D_6/d_8-THF show free THF in solution and the chemical shifts of ligand methyl groups experience significant ring-shielding which can only occur from aryl rings on adjacent ligands. Both features point to conversion to higher-order aggregates when the THF concentration is reduced. Recrystallization of the materials from hydrocarbon solutions results in secondary laddering as tetrameric Li_4O_4 clusters with a cuboidal core, three examples of which have been crystallographically characterised. These clusters are relatively insoluble and melt up to 250 °C; a consideration of the solid-state structures indicates that the clusters with 2,6-diisopropylphenyl substituents form very uniform ball-like molecular structures that will only be weakly solvated.

Keywords: β-ketoimine; β-ketoiminate; lithiation; high-nuclearity clusters; crystallography; DFT calculations; X-ray crystallography; multinuclear NMR; primary laddered units; secondary laddering

1. Introduction

Transition metal complexes of the deprotonated ligands derived from β-ketoimines **1** are of current interest in coordination chemistry and catalysis. Much of their use in catalysis has been in olefin polymerization [1,2]. Lanthanide alkoxides stabilized by β-ketoiminates are active in ring-opening polymerization of lactones and lactides [3]. Some research has been done into other types of reactions [4], and metal complexes of β-ketoimines have been widely used as precursors for metalloorganic chemical vapour deposition (CVD) [5,6]. Much less is known about their main group metal derivatives, although β-ketoiminate complexes of aluminium are a notable exception [7,8]. A few magnesium complexes have also been studied with interest in their use as CVD precursors [9]. Alkali metal derivatives have been used as intermediates in the synthesis of transition metal complexes [10,11], but have not been extensively reported as isolated species [12–14].

The structural chemistry of lithiated organoelement species has seen enormous development over 30 years of active investigation and is known to show great diversity of structures due to aggregation

and Lewis base coordination. Rings, ladders and higher aggregates have been obtained [15–18]. To date, there are several structurally characterised examples of lithium β-ketoiminates. Lithiation of 4-isopropylaminopent-3-en-2-one generates in presence of hexamethylphosphortriamide (hmpa) a *transoid* Li_2O_2 chelate dimer of type **2** (Cambridge Crystallographic Database, CSD, refcode NOWHUK) while in absence of the Lewis base an Li_4O_4 chelated tetrameric cubane (refcode: NOWHOW) of type **3** [12]. A fluorinated β-ketoiminate with a pendent $Me_2N'CH_2CH_2$ has been structurally characterised (refcode: XUZWOE) as a *cisoid* Li_2O_2 dimer with the *N*' donors acting as an internal Lewis base [19], while a mixed copper-lithium ladder cluster was obtained from lithiated **1a** and copper(I) chloride in toluene in which an oxygen from the copper chelate acts as "L" [20]. A similar Li_2O_2 cluster (refcode: SEKVIK) of a close analogue of ligand **1b** (2,6-xylyl rather than Mes group) has two neutral ligands filling the coordination sphere of the lithium ions [21]. An iron(II) triflate complex derived from **1a** (refcode: ISEXUA) has recently been structurally characterised [22]. Titanium chloride and chloromethyltin complexes (refcodes: LIRCAQ and DULREI) of **1b** have also been structurally confirmed [23,24]. Similar chloroalklytin complexes of **1c** have been reported [25]. Main group element complexes of **1d** have also been structurally characterised ($GaCl_3$, refcode: RUYSIO and $SbCl_3$, refcode: JOHQED) [26,27], as have complexes of this ligand with cobalt, copper and europium (refcodes: WUWDUO, WUWFAW, WUWFEA) [28].

As a continuation of our interest in heteroallyl ligands incorporating bulky substituents and their coordination chemistry [29–33], as well as in the structures and reactivities of *N*′-imidoylcarboximidamides [34,35], we now report crystal structures for two popular β-ketoimines **1a**,**b** (Dipp = 2,6-diisopropylphenyl; Mes = 2,4,6-trimethylphenyl) (Scheme 1) [36] and the synthesis of two less-common analogues which have an additional methyl group at the "3" position of the heteropentadienes **1c**,**d**. The structures of new *transoid* Li_2O_2 dimers **2a**–**c** with L = THF and novel D_2-symmetric Li_4O_4 cubanes **3b**–**d** are described. The relationship between dimeric and tetrameric aggregates and the preference for the common S_4- and rare D_2-symmetric Li_4O_4 cubanes is rationalised using hybrid-DFT calculations. We have recently reported the structure of the first mixed ketoiminate-alkyl complex of magnesium derived from **1b** [37].

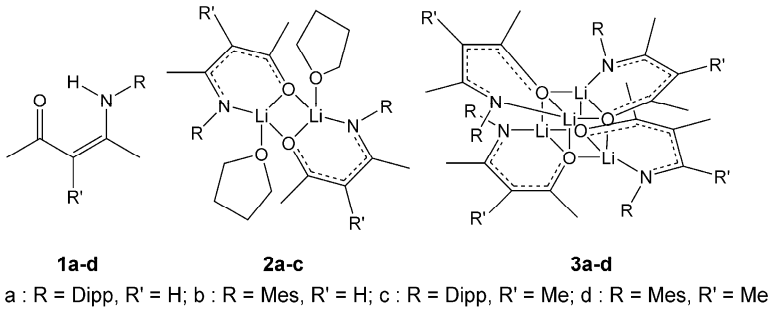

Scheme 1. Identities of the title compounds.

2. Results and Discussion

2.1. Synthesis, Structures and Tautomers of β-Ketoimines

The ketoimines **1c**,**d** were prepared by the $InBr_3$-catalysed condensation of 3-methyl-2,4-pentandione with the corresponding anilines $MesNH_2$ or $DippNH_2$ [38] and have been fully characterised in the solid and in solution; previous reports of these ligands do not seem to have provided full details. The spectroscopic properties resemble those of the previously reported **1a**,**b** [36]. The presence of the intramolecular H-bond is detected by broad resonances in the ^{1}H NMR at noticeably low frequencies (ranging from 11.8 to 13.2 ppm in $CDCl_3$ solution for the four exemplars) [39]. The presence in both **1a** and **1c** of two distinct ^{i}Pr methyl resonances suggesting that there is a lack of free rotation of the Dipp ring is also noteworthy. More interesting are the structures in the solid state

which we have determined for all four species by single-crystal X-ray diffraction at low temperatures (see Figure 1 and Table 1). In each case, an NH hydrogen could be detected unambiguously in the difference Fourier map and their positions and isotropic temperature factors could be freely refined. This suggests that of the three theoretically possible tautomers (Scheme 2), all four ketoimines **1a–d** are unambiguously in the enamine form **B** in the solid state.

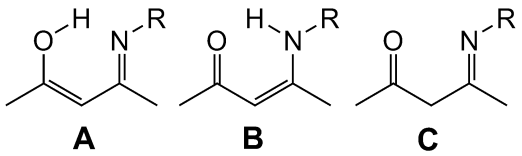

Scheme 2. Limiting tautomers for ketoimines: enol (**A**); enamine (**B**); or ketimine (**C**).

The structure of **1a** (Figure 1a) can be compared to that of (*Z*)-3-((2,6-diisopropylphenyl)amino)-1-phenylbut-2-en-1-one with which it shares an identical value for *d*(N···O) of 2.613(2) Å within experimental error (refcode NAWKUS) [40]. The packing of this structure in regular sheets through weak intermolecular contacts is more symmetrical than that found in **1a**. During this work, another crystal structure of **1a** was published (refcode: UZOJOJ [25]). The geometries of the two structure determinations match closely.

Table 1. Experimental [1] and calculated [2] bond lengths (Å) and angles (°) for **1a–d**.

Parameter	1a		1b		1c		1d	
	X-ray	Calc.	X-ray	Calc.	X-ray	Calc.	X-ray	Calc.
O–C$_2$	1.2506(19)	1.251	1.2408(18)	1.250	1.248(2)	1.252	1.2489(17)	1.252
C$_2$–C$_3$	1.421(2)	1.438	1.426(2)	1.438	1.426(2)	1.450	1.430(2)	1.450
C$_3$–C$_4$	1.376(2)	1.385	1.3827(19)	1.385	1.388(2)	1.395	1.3872(19)	1.395
C$_4$–N	1.3406(19)	1.354	1.3395(18)	1.385	1.349(2)	1.358	1.3462(17)	1.358
C$_7$–C$_3$					1.512(2)	1.517	1.512(19)	1.517
O$_1$–C$_2$–C$_3$	123.16(14)	123.50	122.99(13)	123.47	123.69(16)	123.98	123.35(12)	123.99
C$_2$–C$_3$–C$_4$	123.22(14)	123.04	123.26(13)	123.07	120.18(14)	120.40	120.59(12)	120.46
C$_3$–C$_4$–N	120.46(13)	120.78	121.85(13)	120.99	120.96(16)	120.99	121.93(12)	120.91
C$_4$–N–C$_6$	127.46(13)	126.85	124.92(12)	126.46	120.8(13)	128.03	126.29(11)	128.37
N–H	0.885(19)	1.030	0.860(19)	1.031	0.92(2)	1.032	0.898(17)	1.033
N···O	2.6139(17)	2.647	2.6571(16)	2.652	2.5485(18)	2.590	2.5823(15)	2.591
N–H···O	141.9(16)	138.8	133.7(16)	138.2	140.9(19)	140.1	140.0(15)	140.4
N···O′			2.9840(16)	-				
N–H···O′			136.9(16)	-				

[1] The atom numbering scheme is that shown in Figure 2d. [2] B3LYP/6-31G(d) hybrid DFT.

The structure of **1b** (Figure 1b) is the sole exemplar in this set which shows additional intermolecular H-bonding to form centrosymmetric dimers with respect to crystallographic centres of inversion in space group $P2_1/n$ (see Figure A1 in Appendix A). The intramolecular *d*(N···O) value is 2.657(2) while between the two molecules it is 2.984(2) Å. This motif is strongly reminiscent of that found in 2-(2,6-diisopropylphenylamino)cyclohex-1-enyl phenyl ketone for which the corresponding values are: *d*(N···O) intra- 2.598(3) and 2.614(3); inter-molecular 3.205(3) and 3.206(3) Å. Thus, it is not the difference in steric bulk between the nitrogen substituents Dipp in **1a** and Mes in **1b** that determines these motifs, which are probably determined by crystal packing. During this work, two independent reports were published containing the same structure (refcodes: IFOWUW [41] and NABYEX [42]). The geometries of the three structure determinations match very well.

The isolated structure of **1c** (Figure 1c) has a noticeably short *d*(N···O) value of 2.549(2) Å, 3% less than in **1a**. Similarly, in **1d**, *d*(N···O) is 2.582(2) Å, which is 3% less than in **1b**. The origin of this "pinching-in" effect must lie with the additional backbone methyl group, such that there

are three methyl groups in series along the ketoimine backbone. Although methyl groups are not considered bulky substituents, local steric *pressure* can be generated even by relatively small groups in close proximity [43]. Of about 150 crystal structures of β-ketoimines in the CSD, excluding those cases where two or more of the hetero-pentadiene atoms are constrained within rings, none bear a 3-methyl substituent and only three examples of substitution are found (refcodes: JEKLUA, JEKMAO, and SENBAO), each of which is a perpendicularly-oriented acyl group that is not expected to develop much steric pressure [44,45].

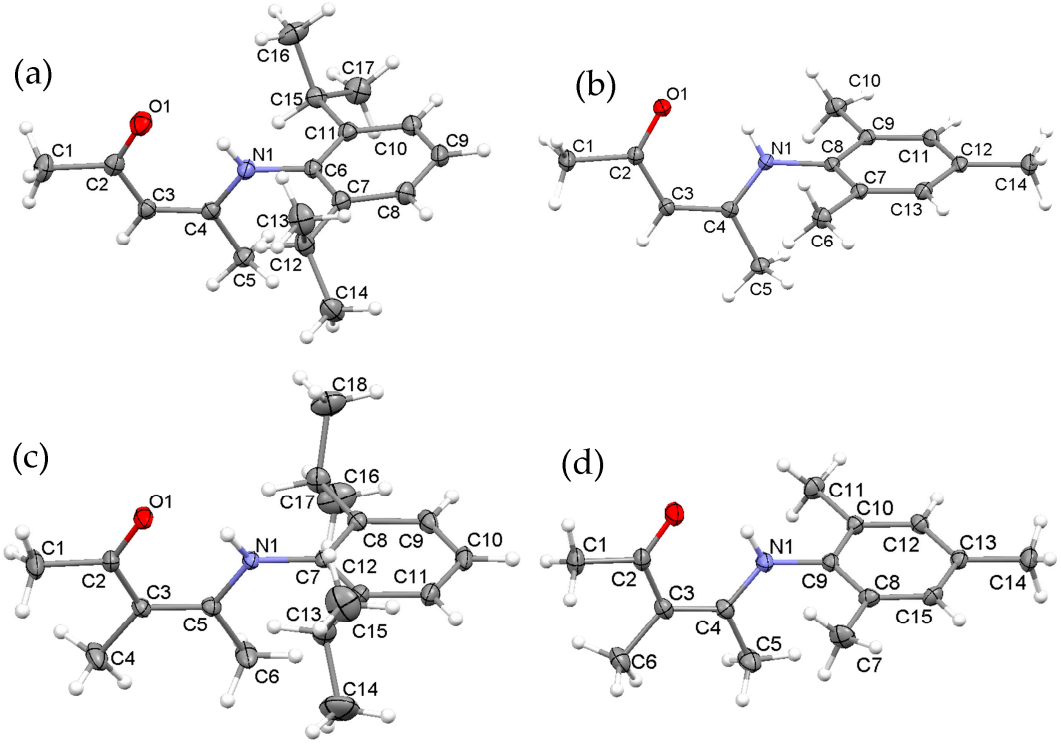

Figure 1. Displacement ellipsoids plots (40% probability) of the molecular structures of the ketoimine ligand precursors as found in the respective crystal structures: (**a**) Ligand **1a**; (**b**) ligand **1b**; (**c**) ligand **1c**; and (**d**) ligand **1d**. The atom numbering schemes are indicated.

In the extended structure of **1c**, the ketoimine chains form into planes that lie along the (020) Miller planes with only weak intermolecular contacts. The observed H-bonding is strictly intramolecular. The same is true of **1d**, but the crystal packing of this exemplar has the molecules arranged such that the aromatic mesityl rings of pairs of molecules are parallel-displaced edgewise at close to the ideal distances for a π–π stacking interaction [46], 3.546 Å from the centre of one mesityl to the plane made by the other and with an average edgewise displacement of 1.337 Å.

For all these β-ketoimines the H-bonded *pseudo* six-member rings are rigorously planar and there is a degree of bond averaging suggestive of at least partly-delocalized π-electrons with sp^2-hybridized 2nd-row elements (Table 1). Thus, the C–N bonds are considerably shorter than expected for a single bond (Av. 1.339 Å) while the formal C=C double bond (Av. 1.316 Å) prescribed by the enamine structure is significantly shorter than that found. Similarly, the formal C–C single bond (Av. 1.530 Å) is not observed; instead the value is typical of single bonds in conjugated systems (Av. 1.460 Å), while the C=O bond is longer than normal values for ketones (Av. 1.210Å) [47].

The geometry of these structures is accurately reproduced by (gas phase) B3LYP/6-31G(d) calculations (Table 1) except for the C(2)–C(3) distances in **1c**,**d** which are overestimated by 0.02 Å. The DFT calculations closely replicate the shortening of *d*(N···O) by ~0.1 Å, supporting the notion that steric crowding of the backbone methyl groups causes the ring to pinch in. Recent computational

studies on a model β-ketoimine **1** with substituents $R_1 = R_2 = R_4 = CH_3$; $R_2 = H$ provides strong support for the preference for the enamine tautomer and moreover has demonstrated that the main factor favoring the enamine is promotion of planarity of the N atom so that its lone pair can be part of a delocalized π-system [48].

2.2. Synthesis and Structures of Ketoiminate Lithium Complexes

The neutral lithium complexes formed by deprotonation of **1a**–**d** with ^{n}BuLi fall into two broad classes: **2a**–**c** which are prepared in and crystallised from THF-hexane mixed solvents and which retain coordinated THF; **3b**,**c** which are prepared in heptane-hexane mixed solvents and which crystallise as unsolvated species. In this system, **3d** stands out in that it preferentially crystallises as the unsolvated cluster even in presence of THF. X-ray quality crystals of **2a**–**c** and **3d** form on cooling from a THF-enriched solution; **3b** recrystallizes from hot toluene, and **3c** from hot heptanes.

2.2.1. *Transoid* Li_2O_2 Clusters

Each of the THF solvates **2a**–**c** consists of a ketoiminate chelated Li^+ ion further coordinated by one THF perpendicular to the chelate ring (Figure 2 and Table 2); these rings associate into crystallographically centrosymmetric dimers with central Li_2O_2 squares that are close to symmetrical with the "inter-monomer" Li–O distances (**2a** 1.917(4); **2b** 1.948(3); **2c** 1.898(2) and 1.908(2) Å) only 1%–3% longer than the "intra-monomer" (**2a** 1.899(3); **2b** 1.888(3); **2c** 1.868(3) and 1.867(2) Å) values. The result is that each Li^+ ion is tetracoordinate but with angles severely distorted from tetrahedral values. There are no significant short contacts between any of these butterfly clusters within their unit cells. For **2c**, the lattice has two crystallographically independent "monomers" in the asymmetric unit, each of which is dimerized on a lattice inversion centre. The two resultant dimers, which are crystallographically distinct, have very comparable geometric parameters and only one example is shown in Figure 2c.

Table 2. Experimental [1] and calculated [2] bond lengths (Å) and angles (°) for **2a**–**d**.

Parameter	2a		2b		2c		2d
	X-ray	Calc.	X-ray	Calc.	X-ray	Calc.	Calc.
O–C$_2$	1.2860(19)	1.290	1.283(2)	1.291	1.284(1)	1.289	1.292
C$_2$–C$_3$	1.372(2)	1.390	1.377(2)	1.390	1.385(4)	1.403	1.402
C$_3$–C$_4$	1.431(2)	1.437	1.432(2)	1.435	1.450(1)	1.451	1.451
C$_4$–N	1.301(2)	1.312	1.306(2)	1.312	1.307(0)	1.317	1.315
C$_7$–C$_3$					1.523(2)	1.524	1.523
Li–N	2.021(3)	2.065	2.016(3)	2.022	2.022(2)	2.041	2.007
Li–O chelate	1.899(3)	1.912	1.888(3)	1.902	1.868(1)	1.882	1.881
Li–O bridge	1.917(3)	1.939	1.948(3)	1.960	1.903(7)	1.947	1.947
Li–O(THF)	1.988(3)	2.040	1.991(3)	2.016	1.98(2)	2.037	2.026
O–C$_2$–C$_3$	125.34(16)	125.76	125.57(16)	125.81	125.47(4)	125.47	125.32
C$_2$–C$_3$–C$_4$	128.68(16)	128.79	128.08(16)	128.20	123.66(11)	124.11	123.75
C$_3$–C$_4$–N	122.86(15)	123.90	123.40(16)	123.50	123.66(15)	124.15	123.82
C$_4$–N–C$_6$	120.58(14)	121.48	118.78(14)	122.10	120.76(9)	121.76	122.27
O–Li–N	95.96(13)	96.58	96.49(13)	97.03	92.28(6)	92.98	92.99
Li–O–Li	85.89(13)	85.76	86.52(13)	85.57	88.1(15)	86.73	85.74
O–Li–O	94.11(13)	94.24	93.48(13)	94.43	92.0(15)	93.27	94.26
O–Li–O(THF)	107.6(11)	107.81	112(9)	111.02	108(3)	108.96	112.06
C$_4$–N–Li	121.68(14)	119.82	121.33(14)	121.29	122.92(8)	122.59	123.92
C$_2$–O–Li	123.68(14)	123.27	124.39(14)	123.70	126.68(19)	127.04	127.13

[1] The atom numbering scheme is that shown in Figure 2d. [2] B3LYP/6-31G(d) hybrid DFT.

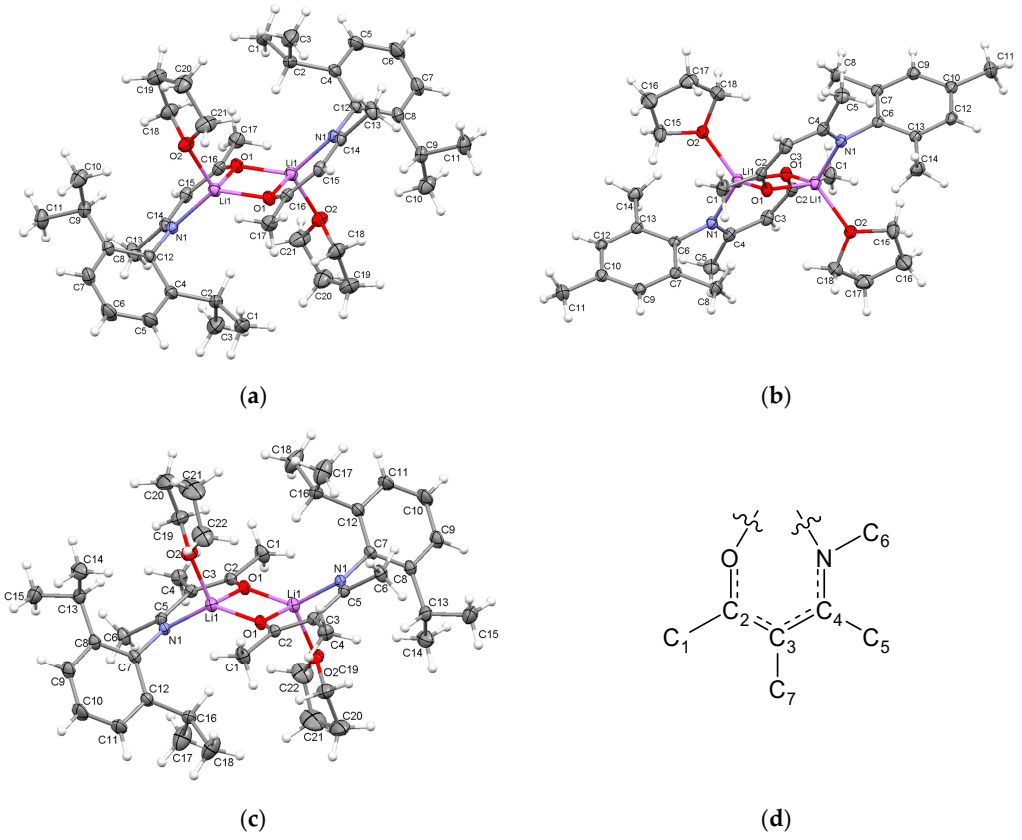

Figure 2. Displacement ellipsoids plots (40% probability) of the centrosymmetrically dimerized molecular structures of *transoid* Li_2O_2 square clusters as found in their crystal structures: (**a**) THF-solvated cluster **2a**; (**b**) THF-solvated cluster **2b**; and (**c**) one of two independent THF-solvated clusters of **2c**; (**d**) The atom numbering scheme is the same used in Tables 1–3 for geometrical comparisons.

The influence of the extra backbone methyl group in **2c** is evident in these lithiated derivatives just as is the case for **1c**,**d**. Thus, the *d*(N···O) values of 2.805(1) and 2.809(1) Å are 4% shorter than those that pertain in **2a**, 2.913(2) and **2b**, 2.914(2) Å, due to "pinching in" of the chelate ring. This can also be seen by the fact that the Li atom is twice as far out of the chelate ring ligand least-squares plane (0.44 Å) compared to **2a** (0.24 Å). Upon coordination to Li^+, the bond lengths within the ketoiminate ligands change in predictable fashion. Thus, the C–O distances lengthen ~3%, C_2–C_3 shorten by ~4%, C_3–C_4 lengthen by ~4% and C_4–N shorten by ~3%. All these changes are consistent with conversion from a limiting enamine geometry **B** towards a delocalized chelate ring.

There are several comparable Li_2O_2 butterfly complexes of ketoiminate ligands in the literature. The most comparable structures to **2a**–**c** are the all-aliphatic complex bis((μ_2-*N*-isopropyl-2,4-dimethyl-1-oxa-5-azapenta-2,4-dienyl)-hexamethylphosphoramido-lithium (refcode: NOWHUC) which has hmpa oxygen donors in place of THF [12] and three closely-similar bis(μ_2-3-((aryl)imino)-1-phenylbut-1-en-1-oxy)-bis(tetrahydrofuran)-di-lithium complexes reported by Liu et al. (refcodes: SIYDAH, SIYDEL, SYDIP) [14]. In NOWHUC, the intra- (1.892) and inter-"monomer" (1.955 Å) Li–O distances are most similar to those in **2b**. In the structure of a 2,6-xylyl ketoiminate a structure very similar to that in **2b** is found (refcode: SEKVIP) [21]. In place of the two THF molecules, two neutral ligand molecules are coordinated to lithium ions via the carbonyl oxygen donors. The dimensions in this structure are very close to those in **2b**, except for the Li–O distances which are longer (0.024 Å) for the ligand O and shorter for the exocyclic value (0.012 Å).

2.2.2. "Tetrameric" Cuboidal Clusters

All three cubane complexes **3b–d** adopt the same basic geometry with minor distortions in which the core geometry has approximate D_2 point-group symmetry (Figure 3a). The CSD reports 21 Li_4O_4 cuboidal clusters with nitrogen donors coordinated to Li. Seven of these are either non-chelating or have higher denticity. Of the remainder, eleven adopt the S_4 geometry while only two have the D_2-symmetric structure (Scheme 3).

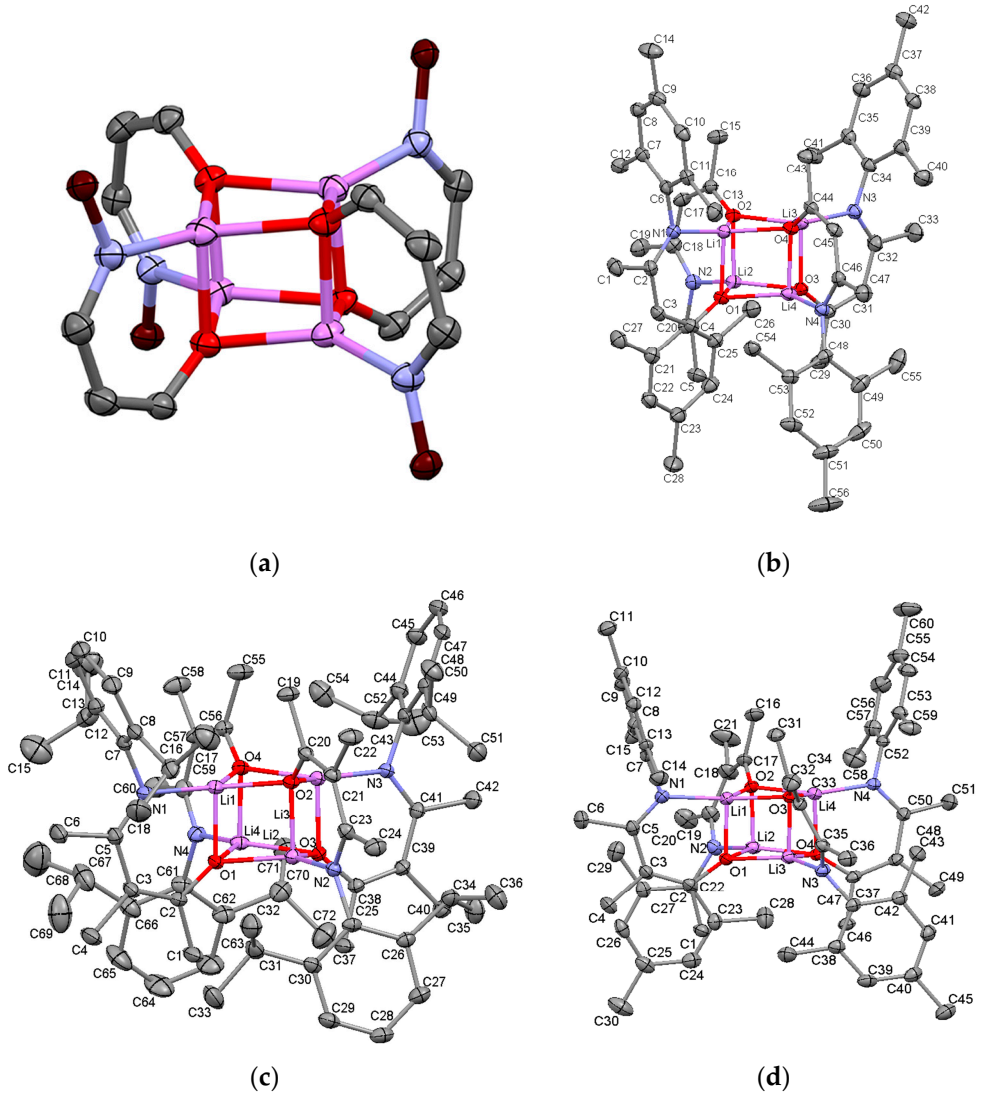

Figure 3. Displacement ellipsoids plots (40% probability) of the tetrameric molecular structures of cuboidal Li_4O_4 ketoiminate clusters as found in their crystal structures: (**a**) common cuboidal core with *ipso* carbon of the aromatic groups coloured brown; (**b**) cluster **3b**; (**c**) cluster **3c**; and (**d**) cluster **3d**. The atom numbering schemes are shown. H atoms on C have been omitted to enhance visualization of the clusters. A disordered, uncoordinated toluene molecule present in the lattice of **3b** has been omitted and solvent presumed to be heptane was removed from the structure of **3c** using the "SQUEEZE" method.

The structure observed in **3b** (Figure 3b and Table 3) is remarkably symmetrical with all the ligand substituents oriented as required by the point group. Two Mes rings attached at opposite corners of the cube are directed away from the cube face and the other two face the opposite direction, each set creating a cavity which in the lattice provide spaces for solvent molecules (toluene). The Li_4O_4 faces perpendicular to the D_2 principal axis are almost square, while the four parallel faces are distinctly

rhomboidal (∠Li–O–Li ~83°). The Li–O distances parallel to the principal axis are precisely those chelated by the ketoiminate ligand and have a mean length of 1.924(5) Å. This is about 3% shorter than the mean Li–O distances for the eight bonds that are not chelated at 1.976(10) Å.

The structure of **3c** (Figure 3c) has the most congested ligand **1c**, with Dipp groups on nitrogen as well as the extra backbone methyl substituent. The same basic high-symmetry geometry is adopted as found for **3b** but the "square" face perpendicular to the principal axis is distinctly distorted into an envelope conformation. This results in the structure being overall much squatter than of the previous example, and not just because of the absence of the substituents at position 4 on the aromatic rings. Here too the four chelated Li–O distances (mean value, 1.874(3) Å) are shorter (by 7%) than the eight bridging distances (mean value, 2.01(4) Å). However, the chelate rings remain close to planar with only a very small deviation of Li out of the average chelate planes. The crystal packing leads to smaller voids but these appear to contain disordered heptane molecules (NMR evidence) which we could not model accurately and which in the end were excluded from the electron-density maps.

Table 3. Experimental [1] and calculated (D_2 and S_4) [2] average bond lengths (Å) and angles (°) for **3a–d**.

Parameter	3a	3b		3c			3d		
	D_2	X-ray	D_2	X-ray	D_2	S_4	X-ray	D_2	S_4
O–C_2	1.305	1.303(2)	1.306	1.310(2)	1.310	1.307	1.310(3)	1.308	1.308
C_2–C_3	1.378	1.366(2)	1.382	1.370(3)	1.392	1.395	1.374(1)	1.392	1.394
C_3–C_4	1.443	1.440(2)	1.442	1.460(7)	1.464	1.461	1.454(2)	1.458	1.457
C_4–N	1.311	1.302(3)	1.308	1.309(2)	1.314	1.318	1.305(4)	1.312	1.314
C_7–C_3				1.524(4)	1.525	1.525	1.522(4)	1.524	1.524
Li–N	2.078	1.988(4)	2.002	2.012(5)	2.056	2.036	1.968(12)	1.983	2.003
Li–O chelate	1.914	1.924(5)	1.931	1.874(3)	1.878	1.881	1.903(15)	1.897	1.887
Li–O bridge	2.026	1.976(10)	1.997	2.01(4)	2.046	2.049	1.98(2)	2.014	2.036
O–C_2–C_3	125.1	125.15(16)	125.3	124.8(4)	124.9	124.91	125.2(3)	125.3	125.5
C_2–C_3–C_4	129.1	127.82(37)	128.9	124.0(3)	124.1	125.32	123.9(6)	124.4	124.7
C_3–C_4–N	124.3	122.77(24)	123.6	123.5(3)	124.8	124.96	123.3(3)	123.8	124.1
C_4–N–C_6	120.7	120.29(98)	121.5	119.1(11)	120.8	120.58	121(1)	122.0	121.4
O–Li–N	96.0	94.77(71)	97.3	91.3(4)	92.3	96.08	92.7(5)	93.9	94.7
Li–O–Li	87.7	85.7(19)	85.8	86(3)	86.5	87.37	84.8(14)	85.4	85.0
O–Li–O	91.9	94(2)	94.0	94(3)	93.2	92.57	95.0(15)	94.4	94.0
C_4–N–Li	120.3	124.1(6)	121.7	125.7(4)	123.6	119.91	123.9(9)	124.8	122.7
C_2–O–Li	125.1	125.1(8)	123.1	130.2(4)	130.0	126.04	125(3)	127.2	125.9

[1] The atom numbering scheme is that shown in Figure 2d. [2] B3LYP/6-31G(d) hybrid DFT.

The structure of **3d** (Figure 3d) is the most distorted of the three by a significant margin. The lithium atoms are distinctly out of the best plane of the ligand atoms, either causing or the result of twisting of the chelate rings. However, here too the four chelated Li–O distances (mean value, 1.903(15) Å) are shorter than the bridging Li–O distances (mean value, 1.98(2) Å) but the difference is only 4%. The chelate rings are twisted away from the principal axis which allows for a smaller ligand bite angle and consequently the Li atoms are 0.494 Å out of the least squares plane generated by the five chelate ring atoms.

The shorter *d*(N···O) values for the clusters derived from the backbone-methyl ligands **1c**,**d** are maintained in the cubane clusters. Thus, the average *d*(N···O) value in **3b** is 2.878(13), in **3c** 2.780(7) and **3d** 2.800(2) Å, which is again shorter by about 3%–4% when using the methylated ligands. Unsurprisingly this is reflected in a smaller average N–Li–O bite angle for the methylated ligands. The bond distances within the chelate rings in **3b–d** become even more averaged than in **2a–c**. The O–C_2 distances are noticeably longer, presumably because the oxygen is now donating to three lithium ions in the cubane. The geometrical parameters are very well simulated in the DFT calculations, which provides substantial confidence that **3a**, for which no crystal structure was obtained, will have a similar geometry.

There are two previously reported ketoiminate Li_4O_4 cluster structures in the CSD. Tetrakis(μ_3-*N*-isopropyl-2,4-dimethyl-1-oxa-5-azapenta-2,4-dienyl)-tetralithium (refcode: NOWHOW)

adopts the S_4-symmetric geometry [12], while tetrakis(μ_3-4-((3-methoxyphenyl)imino)pent -2-en-2-olato)-tetra-lithium (refcode: WUQFAR) adopts the D_2 geometry as observed for **3b**–**d** [13]. These clusters also possess shorter average Li–O distances within the chelate rings (1.905(5) and 1.915(5) Å, respectively) than for the bridging bonds (2.00(2) and 1.961(1) Å).

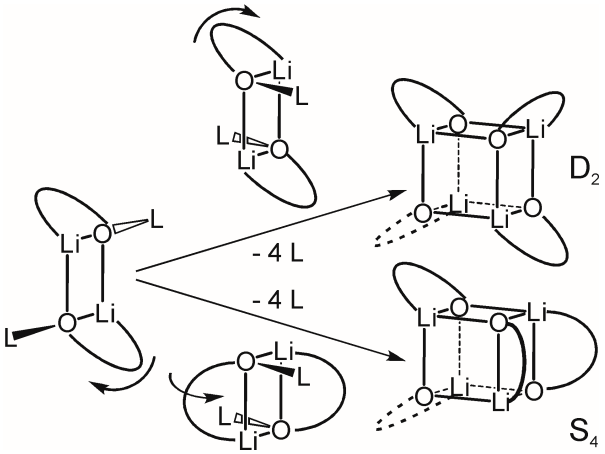

Scheme 3. Dimerization paths of the *transoid* rings of **2** to achieve the known limiting cubane geometries with D_2 or S_4 symmetry. Note that **3b**–**d** all adopt the D_2 geometry.

2.3. Formation and Isomer Selection of Li_4O_4 Clusters

Conceptually, the clusters, whether they adopt the observed D_2 or the much more commonly observed S_4 geometry in the tetramers, are the results of combining the molecular squares discussed above for **2a**–**c**—the primary laddered units [18]—as diagrammed in Scheme 3. Since the dimers are all *transoid*, the face to face combination requires not only the displacement of the two coordinated THF molecules ("L" in Scheme 3) but also folding back of one of the two chelate rings because the observed *cubane* structures contain *cisoid* rings. The possible final geometries are obtained from the Li_2O_2 squares by combining two *cisoid* rings face-to-face, either in register (top) resulting in D_2, or out of register (bottom) yielding S_4. The evidence from synthesis is that formation of the cuboidal clusters is suppressed in THF solution but becomes more favourable on reducing the mole fraction of the coordinating solvent. Note also that the formation of each cubane releases four equivalents of THF, suggesting a likely entropic driving force for the forward reaction.

The evidence from solution NMR obtained in C_6D_6 or 1:1 C_6D_6/THF-d_8 mixtures shows chemical shifts for free THF for **2a**–**c**. Moreover, the NMR spectra of **2b** and **3b** in C_6D_6 are identical. This suggests that in these solvents, the formation of the D_2 cuboidal clusters is favoured. It is furthermore the case that both **3a** and **3c** (in which the aromatic group on N is Dipp) are insoluble in C_6D_6 but soluble in the mixed solvent. By contrast, **3b** and **3d** (with Mes on N) dissolve in C_6D_6. This is contrary to the behaviour of most Dipp compounds, which tend to be very soluble in hydrocarbon solvents. To explain this anomaly, space filling models of the two types of cluster were examined (see Figure A2 in Appendix A). These show a very clear difference in molecule structure, with the Dipp-based structures adopting a very compact spheroidal geometry possessing a very smooth surface that may be difficult to solvate, whereas the Mes-based complexes have large clefts that could be accessed by benzene solvent molecules, aiding solvation.

For confirmation of the hypothesis that the solution forms for all four complexes are the cuboidal Li_4O_4 geometry, consider the coordination chemical shifts for the C1 and C5 methyl groups (see labels in Figure 2d). The C1 methyl group (β to the oxygen atom in the ligand) is shifted to higher frequency by from 0.41 to 0.56 ppm, whereas the C5 group (β to the nitrogen atom) changes little from the free-ligand values. A consideration of the geometries of the *transoid* Li_2O_2 square and cuboidal Li_4O_4 structures indicates that only in the latter do the C1 methyl groups experience significant

ring-shielding from the aryl rings of an adjacent ketoiminate ligand (methyl carbon to ring-centroid distances average in the solid-state structures to 4.557 (**3b**), 4.432 (**3c**) and 3.881 (**3d**) Å. Both the distances and the orientation of the aromatic rings in the *transoid* dimers are markedly less favourable for ring-shielding. Very similar effects and geometrical factors apply for the five-coordinate aluminium *bis* ketoiminates reported by Yu et al. [7]. In four structurally characterised complexes of ligands **1a**,**b** with methyl, ethyl, chloro and fluoro-aluminiums (refcodes BAMFAX, BAMFEB, BAMFIF and BAMFOL, respectively) the average methyl carbon to ring-centroid distances are 3.903, 3.927, 3.904 and 3.912 Å; the corresponding Δδ are +1.17, +1.17, +1.21 and +1.21 ppm (see representative structure diagrams in Figure A3 in Appendix A). The larger ring-shielded shifts are consistent with the short distances and a more favourable orientation over the ring centres in these structures compared to **3b**–**d**. Note that, by contrast, the monomeric dialkylaluminium complexes of ligand **1a** also reported by Yu et al., which cannot experience ring shielding, show no upfield shift compared to the free ligands in the same solvent [7]. The ^{7}Li NMR evidence is less conclusive than that obtained from ^{1}H, although possible time-scale differences make comparisons difficult. There is only one lithium resonance in each case, and the frequencies are quite similar. For the samples measured in 1:1 C_6D_6/THF-d_8, mixture, sharp singlets are observed around +2.5 ppm (**2a**, **2c**, **3b**) but samples in pure C_6D_6 can be sharp (**2b/3b**) or very broad (**2c**, **3d**). Low solubility appears to strongly affect the latter two spectra. Overall, though the presence of **2** ↔ **3** exchange for samples which contain THF cannot be excluded, the dominant species as judged from the ^{1}H NMR signals (C1 methyl and THF peaks) appear to be **3**.

Relatively simple DFT calculations (B3LYP/6-31G(d)) in the gas-phase were undertaken to help explain the observed chemistry. Good matches could be obtained for the geometries of all the ligands and complexes, and the geometries of the missing complexes (**2d**, **3a**) were included computationally (see results compiled in Tables 1–3). Using these computed structures, the energetics of the conversions of **2** to **3** in the gas phase were computed. The outcomes favour **2** over **3** by 104, 99, 133 and 70 kJ·mol^{-1} for **a**–**d**, respectively. Evidently these results do not agree with experiment; the inclusion of solvation energies might change these results, but also the entropy associated with the release of THF molecules in the formation of **3** may be significant.

DFT was also used to help explain the preference for the D_2 over the S_4 geometry for the cuboidal clusters **3**. Such calculations were only undertaken for **3c**,**d** and the corresponding S_4 structures **3c′** and **3d′**. Representative results are shown in Figure 4; the energies calculated for **3c′** and **3d′** are 23 and 41 kJ·mol^{-1} higher than for **3c** and **3d**. A consideration of the optimized computed structures suggests that the origin of the difference is steric as there are significant steric clashes in the S_4 structures that are absent in the preferred D_2 geometries (see Scheme 4).

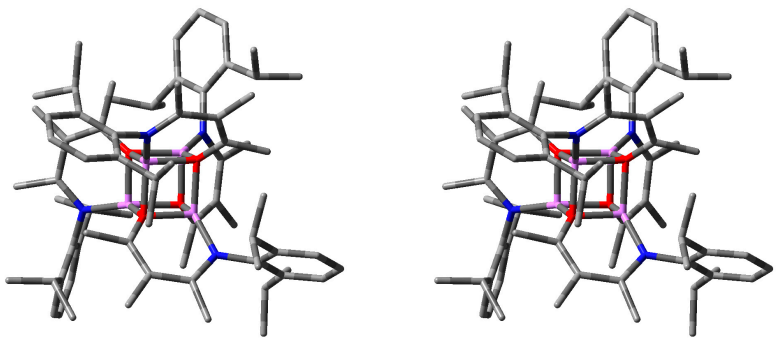

(**a**) (**b**)

Figure 4. DFT calculated structures of **3c**: (**a**) in the crystallographically determined D_2 geometry; and (**b**) in the alternate S_4 geometry (**3c′**). Hydrogen atoms are omitted.

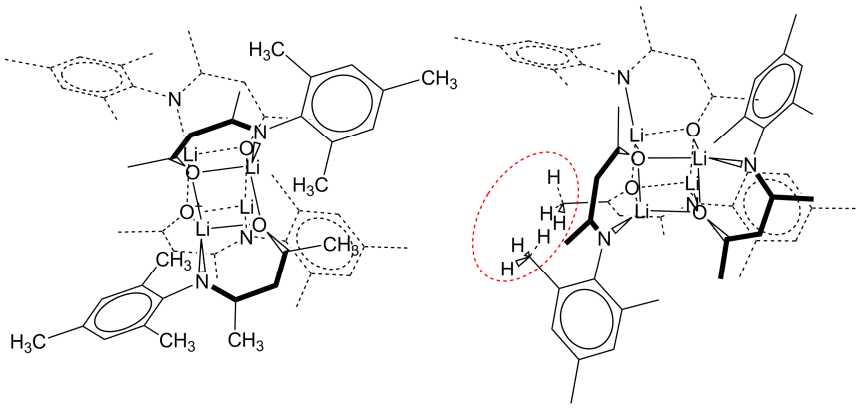

Scheme 4. DFT calculated structures of the *cubane* clusters **3b** with (**left**) D_2 or (**right**) S_4 symmetry imposed. Note the significant steric clashes in the minimized S_4 geometry (dashed red lines).

3. Materials and Methods

3.1. General Methods

All experimental procedures were performed under a nitrogen atmosphere using modified Schlenk techniques, unless otherwise noted. 2,6-Diisopropylaniline, 2,4,6-trimethylaniline, 2,4-pentanedione, 3-methyl-2,4-pentandione, indium tribromide, 1.6 M *n*-butyl lithium in hexane (Aldrich, Saint Louis, MO, USA), aluminium chloride (Merck, Kenilworth, NJ, USA), and benzene-d_6 (CDN Isotopes 0.8 mL ampules) were used as received. Solvents were reagent grade, or better, and were used as received (methanol, hexanes, pentane, chloroform), distilled from sodium/benzophenone (tetrahydrofuran), or obtained from an MBraun Solvent Purification System (heptane, toluene, benzene, methylene chloride). Infrared spectra were recorded on a Bruker Alpha-P diamond ATR spectrometer (East Milton, ON, Canada) as neat samples. ^{1}H, ^{13}C, and ^{7}Li NMR spectra were recorded on a Bruker AvanceII spectrometer operating at 300.13, 75.47 and 116.64 MHz, respectively. HSQC and HMBC were used to assist with assigning the carbon NMR signals where needed. ^{1}H NMR are referenced to tetramethylsilane (TMS), ^{13}C NMR are referenced to $CDCl_3$ or C_6D_6 and ^{7}Li NMR are referenced to an external 9.7 mol/kg LiCl in D_2O solution; coupling constants are expressed in Hz. X-ray crystal data were collected on a Bruker Smart Apex II, with solution and refinement using the *Shelxtl* 6.14 software package. Mass spectra was obtained using a Varian 4000 GC/MS/MS (Palo Alto, CA, USA). Elemental analyses were obtained using an Elementar Vario Micro Cube (Langenselbold, Germany). The ketoimines **1a**,**b** were synthesized by the literature methods [38].

3.2. Synthesis of Ketoimines

3.2.1. 4-((2,6-Diisopropylphenyl)amino)-3-methyl-3-methyl-pent-3-en-2-one **1c**

In a round bottom flask 5.00 g (43.5 mmol) of 3-methyl-2,4-pentandione, 8.85 g (43.5 mmol) 2,6-diisopropylaniline, and 0.154 g (0.435 mmol) of $InBr_3$ were combined and allowed to stir overnight. The cloudy solution was then diluted with 60 mL of distilled water, extracted 3 times with 25 cm^3 of ethyl acetate, the organic layers combined and then dried with magnesium sulphate. The solvent was removed under reduced pressure to give colourless solid and orange liquid. The solid was filtered off and recrystallized from hexanes giving pale yellow plates of **1c** (2.063 g, 17.3%). M.p. 122–129 °C; (Found: C, 78.5; H, 9.6; N, 5.1. $C_{18}H_{27}NO$ requires C, 78.7; H, 9.7; N, 5.4%); ν_{max}(neat)/cm^{-1}: 2960s, 2924m, 2867m, 1598vs, 1555vs, 1464s, 1422s, 1384s, 1352vs, 1262vs, 1235s, 1169s, 1099m, 1053m, 966vs, 814vs, 776vs, 709s, 590m, 445m, 414m. NMR δ(^{1}H, $CDCl_3$, 25 °C): 13.18 (1 H, br s, NH), 7.28 (1H, t, J = 7.44, *para* CH), 7.17 (2H, d, J = 7.44, *meta* CH), 3.01 (2 H, sept, J = 6.87, C*H*CH$_3$), 2.24 (3 H, s, C*H*$_3$C(O)C), 1.92 (3 H, s, C(O)CC*H*$_3$), 1.70 (3 H, s, C(NDipp)C*H*$_3$), 1.18 (6 H, d, J = 6.87, CHC*H*$_3$), 1.14

(6H, d, *J* 6.87, CHCH_3). δ(^{13}C, $CDCl_3$, 25 °C): 196.02 (*C*=O), 161.83 (*C*–N), 146.46 (C_{ortho}), 134.59 (C_{ipso}), 127.96 (C_{para}), 123.62 (C_{meta}), 98.79 (C(O)*C*(CH_3)C), 28.69 (CH_3C(O)C), 28.62 (CHCH_3), 24.65 (CHCH_3), 22.91 (CHCH_3), 16.72 (C(NDipp)CH_3), 14.98 (C(O)CCH_3C); *m/z* (EI) 273 (M^+, 18%), 202 (DippNCCH_3^+, 100%), 187 (DippNC^+, 24%), 160 ($C_{12}H_{16}^+$, 20%).

3.2.2. 4-((2,4,6-Trimethylphenyl)amino)-3-methyl-pent-3-en-2-one **1d**

Procedure as for **1c** from 5.00 g (43.5 mmol) of 3-methyl-2,4-pentanedione, 5.88 g (43.5 mmol) of 2,4,6-trimethylaniline, and 0.154 g (0.4344 mmol) $InBr_3$; removal of the solvent gave an orange liquid from which crystals formed after 2 days. The solid was filtered off and recrystallized from hexanes to give faintly orange plates of **1d** (3.619 g, 36.0%). M.p. 64–68 °C; (Found: C, 77.7; H, 8.8; N, 6.1. $C_{15}H_{21}NO$ requires C, 77.4; H, 8.8; N, 6.4%; ν_{max}(neat)/cm^{-1}: 2947w, 2914w, 2859w, 1595s, 1538vs, 1487s, 1435m, 1417m, 1387m, 1367m, 1350m, 1263vs, 1198s, 1147w, 967vs, 884m, 857s, 814m, 760 m, 696m, 588m, 532w, 482m. NMR δ(^{1}H, $CDCl_3$, 25 °C): 12.99 (1H, br s, NH), 6.89 (2H, s, C*H*), 2.28 (3H, s, *para* CH_3), 2.22 (3H, s, CH_3C(O)C), 2.13 (6H, s, *ortho* CH_3), 1.91 (3H, s, C(O)CCH_3), 1.70 (s, 3H; CH_3 on C(NMes)CH_3). δ(^{13}C, $CDCl_3$, 25 °C): 195.91 (*C*=O), 161.60 (*C*–N), 136.57 (C_{para}), 135.80 (C_{ipso}), 134.91 (C_{ortho}), 128.92 (C_{meta}), 98.85 (C(O)*C*(CH_3)C(NMes), 28.60 (CH_3C(O)C), 21.02 (*para* CH_3), 18.40 (*ortho* CH_3), 16.03 (C(NMes)CH_3), 14.92 (C(O)CCH_3); *m/z* (EI) 232 (MH^+, 100%), 231 (M^+, 30%), 160 (MesNCCH_3^+, 10%).

3.3. Synthesis of the Ketoimide Lithium Complexes

3.3.1. Lithium Ketoiminate Complex **2a**

A solution of 1.006 g (3.878 mmol) of **1a** in 8 mL of dry THF in a Schlenk tube was cooled in an ice/salt bath and 2.5 mL (4.000 mmol) of 1.6 M BuLi in hexanes was added via syringe. Stirring was continued with cooling for 30 min. and then overnight at RT. THF was removed by vacuum until solid started to come out of solution, after which the tube was heated to redissolve the solid and placed in the freezer (−10 °C) to give colourless plates of **2a** (0.322 g, 24.6%) suitable for X-ray crystallography. M.p. 229–230 °C, dec. 270 °C. NMR δ(^{1}H, 1:1 THF:C_6D_6, 25 °C): 1:30 ligand:THF): 7.11 (2H, d, *J* = 7.25, *meta* C*H*), 7.02 (1H, t, *J* = 7.25, *para* C*H*), 4.82 (s, 1 H; backbone C*H*), 3.59 (122 H, m, THF), 3.16 (2H, septet, *J* = 6.82, C*H*CH_3), 1.66 (s, 3 H; CH_3C(O)C), 1.61 (122 H, m, THF), 1.55 (3 H, s, C(NDipp)CH_3), 1.19 (6 H, d, *J* = 6.82, CHCH_3), 1.14 ppm (6 H, d, *J* = 6.82, CHCH_3). δ(^{13}C, 1:1 THF:C_6D_6, 25 °C): 178.48 (*C*–O), 168.22 (*C*N), 148.84 (C_{ipso}), 140.32 (C_{ortho}), 123.72 (C_{para}), 123.52 (C_{meta}), 96.51 (backbone *C*H), 28.60 (CH_3C(O)C), 28.17 (CHCH_3), 24.64 (CHCH_3), 24.56 (CHCH_3), 23.09 (C(NDipp)CH_3). δ(^{7}Li, 1:1 THF:C_6D_6, 25 °C): 2.14.

3.3.2. Lithium Ketoiminate Complex **2b**

Procedure as for **2a** from 1.005 g (4.624 mmol) of **1b** in 9 mL of THF and 3.0 mL (4.800 mmol) of 1.6 M BuLi in hexanes to give colourless blocks of **2b** (0.440 g, 31.2%) suitable for crystallography. M.p. 272–274 °C dec. NMR δ(^{1}H, C_6D_6, 25 °C): 6.84 (2H, s, *meta* C*H*), 5.02 (1H, s, C*H* mesityl), 3.57 (m, 5H, THF), 2.20 (3H, s, *para* CH_3), 2.11 (6H, s, *ortho* CH_3), 1.52 (3H, s, ligand CH_3), 1.49 (3H, s, ligand CH_3), 1.41 (5H, m, THF). δ(^{13}C, C_6D_6, 25 °C): 176.27 (*C*–O), 169.14 (*C*=N), 147.41, 138.22, 132.35, 129.66, 129.28, 128.56, 128.25, 126.03, 99.20 (backbone *C*H), 28.30 (*C*H_3–CO), 22.00 (*para*-*C*H_3), 21.76 (*C*H_3 toluene), 21.32 (CH_3–*C*N), 18.52 (*ortho*-*C*H_3). δ(^{7}Li, C_6D_6, 25 °C): 2.76 ppm.

3.3.3. Lithium Ketoiminate Complex **2c**

Procedure as for **2a** from 0.930 g (3.40 mmol) of **1c** in 10 mL of THF, and 2.2 mL (3.5 mmol) of 1.6 M BuLi in hexanes to give colourless blocks of **2c** (0.333 g 13.9%) suitable for crystallography. m.p. 139–145 °C. NMR δ(^{1}H, 1:1 THF:C_6D_6, 25 °C, containing 1:26 ligand:THF) 7.10 (2H, d, *J* 7.49, *meta* C*H*), 7.00 (1H, t, *J* 7.49, *para* C*H*), 3.59 (106 H, m, THF), 3.11 (2 H, sept, *J* 6.86, C*H*CH_3), 1.85 (3 H, s, C(O)CCH_3), 1.74 (3 H, s, CH_3C(O)C), 1.68 (3 H, s, C(NDipp)CH_3), 1.63 (106 H, m, THF), 1.16 (6 H, d,

J 6.86, CHCH_3), 1.10 ppm (6 H, d, *J* 6.86, CHCH_3). δ(^{13}C, 1:1 THF:C_6D_6, 25C): 175.21 (*C*–O), 169.21 (*C*–N), 149.42 (C_{ipso}), 140.10 (C_{ortho}), 123.59 (C_{meta}), 123.43 (C_{para}), 98.02 (C(O)*C*(CH_3)C), 68.13 (THF), 28.21 (*C*HCH_3), 27.97 (CH_3C(O)C), 26.24 (THF), 24.56 (CH*C*H_3), 24.33 (CH*C*H_3), 21.73 (C(NDipp)*C*H_3), 17.85 (C(O)C*C*H_3C). δ(^{7}Li, 1:1 THF:C_6D_6, 25 °C): 1.33; δ(^{7}Li, C_6D_6, 25 °C): 2.76 (br).

3.3.4. Lithium Ketoiminate Complex **3b** Toluene Solvate

A solution of 0.997 g (4.59 mmol) of **1b** in 10 mL of heptane at 0 °C was treated with 3.0 mL (4.8 mmol) of 1.6 M BuLi in hexanes and then heated to 70 °C to dissolve all solids. After removal of solvent in vacuum, the residue was dissolved in a minimum amount of boiling toluene and placed in the freezer (−10 °C) to give colourless blocks of **3b-C_7H_8** suitable for X-ray crystallography (m.p. 245–250 °C dec.) The NMR data showed that the crystals lost some of the toluene over time to reduce to a ratio of 0.4:1. The elemental analysis was performed during the same week as the NMR was performed; therefore, the elemental analysis data given are for the 0.4:1 ratio crystal. Found: C, 76.1; H, 8.0; N, 6.0. $C_{58.8}H_{74.8}N_4O_4Li_4$ requires: C, 76.0; H, 8.2; N, 6.0. NMR: δ(^{1}H) (C_6D_6, 25 °C) 7.16–7.00 (2H, m, solvate C_7H_8), 6.84 (2H, s, solvate C_7H_8), 5.02 (1H, s, backbone C*H*), 2.20 (3H, s, solvate C_7H_8), 2.11 (6H, s, *ortho* CH_3), 1.52 (s, 3H, Me on backbone), 1.49 (s, 3H, Me on backbone). δ(^{13}C, C_6D_6, 25 °C): 176.27 (*C*–O), 169.14 (*C*=N), 147.41, 138.22, 132.35, 129.66, 129.28, 128.56, 128.25, 126.03, 99.20 (CH on bb), 28.30 (CH_3–CO), 22.00 (*para*-CH_3), 21.76 (CH_3 toluene), 21.32 (CH_3–CN), 18.52 (*ortho*-CH_3). δ(^{7}Li, C_6D_6, 25 °C): 2.76.

3.3.5. Lithium Ketoiminate Complex **3c** Solvate

Procedure as for **3b** from 0.508 g (1.858 mmol) of **1c** and 1.2 mL (1.92 mmol) of 1.6 M BuLi, heated to 80 °C to dissolve. The reaction was then allowed to cool to room temperature which resulted in the formation of white needle-like crystals (m.p. 124.8–131.8 °C, dec.) suitable for crystallography. These crystals do not dissolve in C_6D_6 at 25 °C; in 1:1 C_6D_6/THF-d_8, the same NMR spectrum is obtained as recorded for **2c**. δ(^{7}Li, C_6D_6, 25 °C): δ = 2.45 (br).

3.3.6. Lithium Ketoiminate Complex **3d**

Procedure as for **2a** from 0.706 g (3.05 mmol) **1d** in 10 mL of THF and 2.0 mL (3.2 mmol) of 1.6 M BuLi in hexanes. After removal of THF in vacuum, the residue was dissolved on heating in 4 mL of heptane and 0.7 mL of dry THF placed in the freezer (−10 °C) to give in yellow crystals of **3d** suitable for X-ray crystallographic study. m.p. 244–250 °C, dec. NMR: δ(^{1}H) (C_6D_6, 25 °C) 6.86 (2H, s, *meta* C*H*), (1H, s, backbone C*H*), 2.21 (3H, s, *para* CH_3), 2.18 (6H, s, *ortho* CH_3), 1.92 (3H, s, backbone CH_3), 1.61 (3H, s, backbone CH_3), 1.56 (3H, s, backbone CH_3). δ(^{13}C, C_6D_6, 25 °C): 172.69, 170.08, 147.83, 132.03, 129.24, 129.07, 127.51, 100.64, 27.36, 21.35, 20.83, 18.25, 17.85. δ(^{7}Li, C_6D_6, 25 °C): +1.44.

3.4. X-ray Crystallography

Crystals of **1a–d**, **2a–c** and **3b–d** were mounted on glass fibres in Paratone™ oil and cooled to 173 K in a cold gas stream of the Bruker Kryoflex apparatus and reflection data were collected on an Apex II CCD area-detector diffractometer. Data collection was controlled by APEX2, cell refinement and data reduction was performed with SAINT-Plus and a multiscan absorption correction was applied in each case using SADABS [49]. The structures were solved with SHELXS97 and refined with SHELXTL [50]. Key crystal and refinement data are reported in Table A1 (Appendix B), while archival data are provided in the ESI as CIF files. H atoms were refined using a riding model with the exception of the N(1)–H atoms in **1a–d** which were refined freely with isotropic temperature factors. The structure of **3b** contains free toluene in the lattice that is disordered in a typical "head-to-tail" fashion [51] with refined occupancy of 78:22 and retains a high degree of thermal motion even at 173 K. Solvent in the lattice of **3c** was even more poorly defined and we ended up subtracting its contribution to the E-density map using the SQUEEZE routine of PLATON (details in the CIF file) [52]. This lattice solvent is the likely source for higher residuals in both the integration and final refinements for this structure;

the model for **3c** itself seems to be robust despite these factors and the "conventional" R-factor (6.54%) is in the normal range. CCDC 1540147–1540156 contain the data deposition for the crystal structures. These data can be obtained, free of charge, via http://www.ccdc.cam.ac.uk/products/csd/request/ (or from the Cambridge Crystallographic Data Centre, 12 Union Road, Cambridge CB2 1EZ, UK (Fax: +44-1223-336033 or e-mail: deposit@ccdc.cam.ac.uk)).

3.5. Computation

DFT calculations for the molecules were done using B3LYP with the 6-31G(d) basis set using Gaussian 03 and visualized with Gaussview 4.1.2 for Windows [53]. All the geometries could be minimized and frequency calculations verified that these are at least local minima for all cases, except for **4c**, for which the geometry never fully converged. The minimized structures are included with the X-ray geometries in the archival CIF file available as ESI.

4. Conclusions

This work reports a detailed structural comparison for two types of ketoiminate complexes of lithium from crystal structures obtained during synthesis. From solutions strongly enriched in THF, *transoid* Li_2O_2 squares are generally obtained, with each lithium cation further coordinated by a THF solvent molecule. Changes in structures of the free ligands and the complexes are observed between the common 3,5-dimethylketomines and the more sterically bulky 3,4,5-trimethylketoimines, with shorter cross-ring O···N distances in free and coordinated chelate rings. More curious was the observation that with ligand **1d**, the cuboidal Li_4O_4 structure is formed in the presence of THF. Similar complexes could be obtained for **3b**,**d** by excluding THF entirely and replacing it with only hydrocarbon solvents. The NMR evidence in either pure deuterated benzene or in benzene/THF mixtures fits for the desolvated cubane structures as the dominant solution species under these conditions. DFT calculations show that the gas-phase energetic preference is for the *transoid* square complexes; however, this does not take the solvation and especially the entropic preference for the desolvated cubanes into consideration. Whereas Dipp and Mes-substituents are generally regarded as quite similar, the structures of the cuboidal clusters show significant differences between clusters formed from the two classes of ligands. The unexpectedly low solubility of the Dipp derivatives seems to be correlated with a more uniform cluster geometry and a very smooth, unbroken, surface. These results, which contradict the normal solubility trends for Dipp- and Mes-derivatives, will be of interest to those wishing to use the lithium salts as reaction intermediates for ligand transfer to other metals: these lithium β-ketoiminates are likely to be considerably more reactive when produced and handled in donating solvents such as THF than if they are prepared for use in a non-polar and non-coordinating solvent. With regards to functional properties, it would appear that the *external* ligand "sheathing" effects can play significant roles and should not be ignored by an undue focus on just the common Li_4O_4 core structures.

Supplementary Materials: The following are available online at www.mdpi.com/2304-6740/5/2/30/s1, electronic file in CIF format with crystal coordinate data for **1a–d**, **2a–c**, **4b–d**, and DFT optimized geometries from B3LYP/6-31G(d) calculations for **1a–d**, **2a–d**, **3a–d** and **3c′**, **3d′** computed with the alternative S_4 geometry.

Acknowledgments: We thank the Natural Sciences and Engineering Research Council (Canada) for funding. The diffractometer was purchased with the help of NSERC and the University of Lethbridge. We thank A. Elizabeth Baker for providing valuable assistance and Tony Montina who provided support and training for the high-field NMR experiments. No funding for open access publishing was received.

Author Contributions: Twyla Gietz and René T. Boeré conceived and designed the experiments; Twyla Gietz performed the experiments; Twyla Gietz and René T. Boeré analyzed the data; and Twyla Gietz and René T. Boeré wrote the paper.

Conflicts of Interest: The authors declare no conflict of interest.

Appendix A

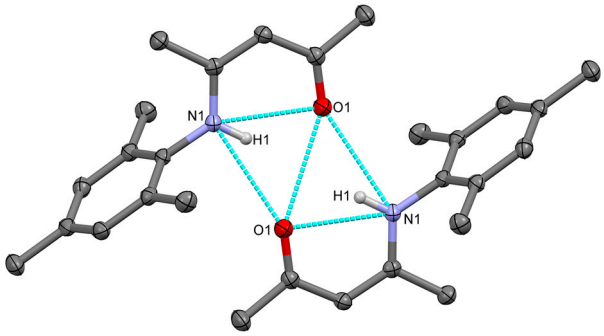

Figure A1. Depiction of the hydrogen-bonding that forms a centrosymmetric dimer in the structure of **1b**. The dihedral angle between the N_1–O_1–N_1'–O_1' and the O_1–C_2–C_3–C_4–N_1 planes is only 16.5°.

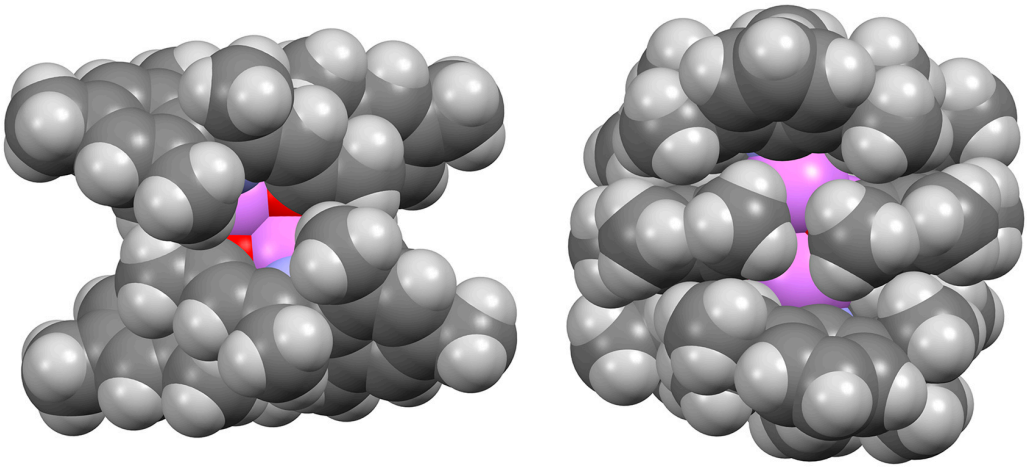

(**a**) (**b**)

Figure A2. Space-filling depictions of the cuboidal Li_4O_4 ketoiminate clusters (**a**) **3b** and (**b**) **3c**, emphasizing the globular nature of the latter and the more angular and clefted nature of the former.

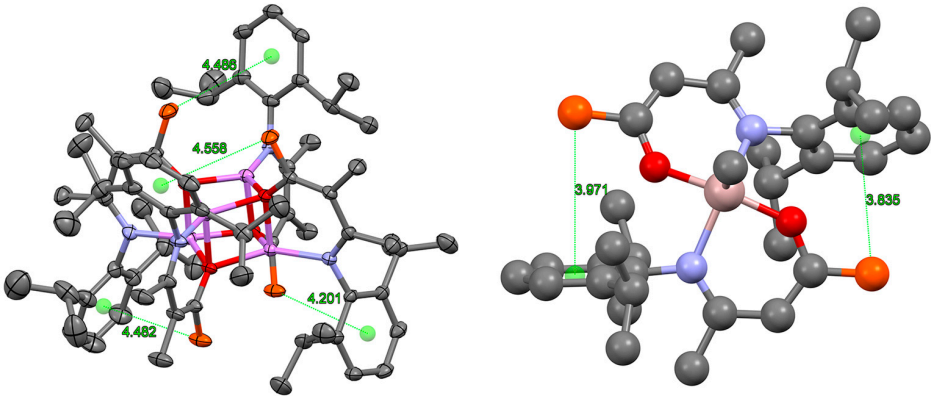

(a) **(b)**

Figure A3. Orientation and distance of ketoiminate methyl carbon atoms (coloured orange) to aryl ring centroids (light green) of the *adjacent* ligands. Contrast the longer distances and poorer orientation in (**a**) **3b** with the more favourable situation in (**b**) the structure with the refcode BAMFAX (see [7]).

Appendix B

Table A1. Crystal data, structure collection and refinement data for X-ray crystallography [1].

(A)

Parameter	1a	1b	1c	1d
Formula	$C_{17}H_{25}NO$	$C_{14}H_{19}NO$	$C_{18}H_{27}NO$	$C_{15}H_{21}NO$
FW, amu	259.38	217.30	273.41	231.33
T, K	173(2)	173(2)	173(2)	173(2)
λ, Å	0.71073	0.71073	0.71073	0.71073
Crystal system	orthorhombic	monoclinic	orthorhombic	monoclinic
Space group	*Pccn*	$P2_1/n$	$P2_12_12_1$	$C2/c$
Cell: *a*, Å	12.3641(12)	10.0068(6)	6.7423(4)	18.8762(17)
b, Å	16.3858(16)	9.8961(6)	13.9706(8)	8.0097(7)
c, Å	15.4945(15)	12.7933(8)	18.0631(10)	19.0037(17)
α, °	90	90	90	90
β, °	90	99.1380(10)	90	107.5430(10)
γ, °	90	90	90	90
V, Å^3	3139.1(5)	1250.82(13)	1701.44(17)	2739.6(4)
Z	8	4	4	8
D_{calc}, g/cm^3	1.098	1.154	1.067	1.112
μ, mm^{-1}	0.067	0.072	0.065	0.069
F(000)	1136	472	600	1008
Cryst. size, mm^3	0.54 × 0.41 × 0.20	0.27 × 0.25 × 0.14	0.42 × 0.20 × 0.14	0.43 × 0.34 × 0.16
θmin, max, °	2.06, 26.73	2.41, 27.10	1.84, 27.40	2.25, 27.48
h min, max	−15, 15	−12, 12	−8, 8	−24, 24
k min, max	−20, 20	−12, 12	−18, 18	−10, 10
l min, max	−19, 19	−16, 16	−23, 23	−24, 24
Rfl_{all}	40165	17205	24505	19053
Rfl_{indep}, R_{int}	3338, 0.0561	2762, 0.0254	2224, 0.0285	3153, 0.0240
Compl., θ, °	100, 26.73	99.9, 27.10	100, 25.25	99.9, 27.48
Abs corr.	semi-empirical from equivalents			
Max/min trans.	0.9868, 0.9646	0.9914, 0.9378	0.9916, 0.9279	0.9918, 0.9169
Data	3338	2762	2224	3153
Restraints	0	0	0	0
Parameters	182	153	191	163
GOF	1.032	1.047	1.031	1.053
R_1 ($I > 2\sigma I$)	0.0428	0.0462	0.0407	0.0465
wR_2 (all data)	0.1201	0.1349	0.1172	0.1402
Max, min, e·Å^{-3}	0.20, −0.21	0.26, −0.31	0.20, −0.18	0.26, −0.22

(B)

Parameter	2a	2b	2c
Formula	$C_{42}H_{64}Li_2N_2O_4$	$C_{36}H_{52}Li_2N_2O_4$	$C_{44}H_{68}Li_2N_2O_4$
FW, amu	674.83	590.68	702.88
T, K	173(2)	173(2)	173(2)
λ, Å	0.71073	0.71073	0.71073
Crystal system	triclinic	monoclinic	monoclinic
Space group	$P\bar{1}$	$P2_1/c$	$P2_1/n$
Cell: *a*, Å	9.4060(8)	8.0148(5)	20.843(5)
b, Å	10.7931(9))	15.0628(9)	10.495(2)
c, Å	11.9959(10)	14.5918(9)	21.365(5)
α, °	69.0400(10	90	90
β, °	73.6160(10)	103.8550(10)	112.886(2)
γ, °	67.0160(10)	90	90
V, Å^3	1032.50(15)	1710.35(18)	4305.7(17)
Z	1	2	4
D_{calc}, g/cm^3	1.085	1.147	1.084
μ, mm^{-1}	0.067	0.073	0.067
F(000)	368	640	1536

Table A1. *Cont.*

(B)

Parameter	2a	2b	2c
Cryst. size, mm^3	0.36 × 0.20 × 0.12	0.39 × 0.18 × 0.11	0.46 × 0.19 × 0.17
θmin, max, °	1.84, 26.03	1.97, 27.48	1.75, 27.48
h min, max	−11, 11	−10, 10	−27, 27
k min, max	−13, 13	−19, 19	−13, 13
l min, max	−14, 14	−18, 18	−27, 27
Rfl_{all}	10854	19537	60577
Rfl_{indep}, R_{int}	4040, 0.0245	3919, 0.0373	9865, 0.0250
Compl.,%; θ, °	99.6, 25.25	100.0, 25.25	99.9, 27.48
Abs corr.	semi-empirical from equivalents		
Max/min trans.	0.9918, 0.9136	0.9916, 0.8956	0.9918, 0.9266
Data	4040	3919	9865
Restraints	0	0	0
Parameters	232	204	483
GOF	1.035	1.025	1.030
R_1 ($I > 2\sigma I$)	0.0464	0.0495	0.0453
wR_2 (all data)	0.1274	0.1409	0.1285
Max, min, $e{\cdot}Å^{-3}$	0.23, −0.19	0.24, −0.25	0.32, −0.21

(C)

Parameter	3b	3c	3d
Formula	$C_{56}H_{72}Li_4N_4O_4{\cdot}C_7H_8$	$C_{72}H_{104}Li_4N_4O_4$	$C_{60}H_{80}Li_4N_4O_4$
FW, amu	985.07	1117.35	949.04
T, K	173(2)	173(2)	173(2)
λ, Å	0.71073	0.71073	0.71073
Crystal system	orthorhombic	monoclinic	monoclinic
Space group	$P2_12_12_1$	$P2_1/n$	$P2_1/n$
Cell: *a*, Å	13.7530(9)	14.3398(14)	13.0543(11)
b, Å	18.3062(13)	27.504(3)	26.647(2)
c, Å	24.0904(17)	19.8735(19)	16.4965(14)
α, °	90	90	90
β, °	90	107.4870(10)	91.2180(10)
γ, °	90	90	90
V, $Å^3$	6065.1(7)	7475.9(13)	5737.1(8)
Z	4	4	4
D_{calc}, g/cm^3	1.079	0.993	1.099
μ, mm^{-1}	0.065	0.059	0.067
F(000)	2120	2432	2048
Cryst. size, mm^3	0.48 × 0.40 × 0.24	0.69 × 0.27 × 0.13	0.40 × 0.22 × 0.22
θmin, max, °	1.69, 27.48	1.66, 25.03	1.75, 27.48
h min, max	−17, 17	−17, 17	−16, 16
k min, max	−23, 23	−32, 32	−34, 34
l min, max	−31, 31	−23, 23	−21, 21
Measured rfl	70155	88683	82309
Indep. rfl, R_{int}	7604 0.0372	13200, 0.0921	13161, 0.0572
Compl.,%; θ, °	100.0, 25.25	100.0, 25.03	100.0, 27.48
Abs corr.	semi-empirical from equivalents		
Max/min trans.	0.9842, 0.9692	0.9918, 0.8738	0.9843, 0.9016
Data	7604	13200	13161
Restraints	84	0	0
Parameters	762	785	673
GOF	1.039	0.985	1.011
R_1 ($I > 2\sigma I$)	0.0386	0.0654	0.0532
wR_2 (all data)	0.1077	0.1786	0.1478
Max, min, $e{\cdot}Å^{-3}$	0.21, −0.16	0.25, −0.19	0.26, −0.19

[1] See deposited CIF files for full data.

References

1. Cho, M.H.; Yoon, J.S.; Lee, I.M. Efficient bimodal ring-opening polymerization of ε-caprolactone catalyzed by titanium complexes with *N*-alkoxy-β-ketoiminate ligands. *Bull. Korean Chem. Soc.* **2007**, *28*, 2471–2476.
2. Wang, L.Y.; Wu, Q. Ethylene polymerization catalyzed by Pd-based β-ketoiminato complexes/MAO systems. *Eur. Polym. J.* **2007**, *43*, 3970–3975. [CrossRef]
3. Peng, H.; Zhang, Z.; Qi, R.; Yao, Y.; Zhang, Y.; Shen, Q.; Cheng, Y. Synthesis, reactivity, and characterization of sodium and rare-earth metal complexes bearing a dianionic *N*-aryloxo-functionalized β-ketoiminate ligand. *Inorg. Chem.* **2008**, *47*, 9828–9835. [CrossRef] [PubMed]
4. Lee, D.H.; Cho, M.H.; Kwon, I.H.; Jun, I.C.; Lee, I.M.; Jin, M.J. Palladium phosphanyl-β-ketoiminate complexes as highly active catalysts for Heck coupling reaction. *Catal. Commun.* **2008**, *9*, 1517–1520. [CrossRef]
5. Lim, S.W.; Lee, J.C.; Shon, D.S.; Lee, W.I.; Lee, I.M. A study on the development of chemical vapor deposition precursors. 4. Syntheses and characterization of new *N*-alkoxo-β-ketoiminate complexes of niobium and tantalum. *Chem. Mater.* **2002**, *14*, 1548–1554. [CrossRef]
6. Lim, S.W.; Choi, B.; Min, Y.S.; Lee, S.S. A study on the development of CVD precursors V—Syntheses and characterization of new *N*-alkoxy-β-ketoiminate complexes of titanium. *J. Organomet. Chem.* **2004**, *689*, 224–237. [CrossRef]
7. Yu, R.C.; Hung, C.H.; Huang, J.H.; Lee, H.Y.; Chen, J.T. Four- and five-coordinate aluminum ketiminate complexes: Synthesis, characterization, and ring-opening polymerization. *Inorg. Chem.* **2002**, *41*, 6450–6455. [CrossRef] [PubMed]
8. Kuo, P.C.; Chen, I.C.; Chang, J.C.; Lee, M.T.; Hu, C.H.; Hung, C.H.; Lee, H.M.; Huang, J.H. Hydroalumination of carbon dioxide, carbon disulfide, and phenyl isocyanate with an aluminum ketiminate compound. *Eur. J. Inorg. Chem.* **2004**, *24*, 4898–4906. [CrossRef]
9. Ouattara, T.S.; Butcher, R.J.; Matthews, J.S. Synthesis and characterization of bis[4-*N*-(cyclohexylimino)-2-pentanonato]magnesium(II). *J. Coord. Chem.* **2005**, *58*, 461–465. [CrossRef]
10. Jones, D.; Roberts, A.; Cavell, K.; Keim, W.; Englert, U.; Skelton, B.; White, A. Synthesis of new adducts and co-ordination complexes of zirconium and titanium containing β-aminoketone ligands. Crystal structures of isostructural adducts MCl4·2Pr^{i}HNCMe=CHCMe=O (M = Ti or Zr) and the complex [Zr(PhNCMe =CHCMe=O)$_2$Cl$_2$]. *J. Chem. Soc. Dalton Trans.* **1998**, *2*, 255–262. [CrossRef]
11. Hsu, S.; Chang, J.; Lai, C.; Hu, C.; Lee, H.M.; Lee, G.; Peng, S.; Huang, J. Terminal titanium-ligand multiple bonds. Cleavages of CdO and CdS double bonds with Ti imido complexes. *Inorg. Chem.* **2004**, *43*, 6786–6792. [CrossRef] [PubMed]
12. Brehon, M.; Cope, E.K.; Mair, F.S.; Nolan, P.; O'Brien, J.E.; Pritchard, R.G.; Wilcock, D.J. Structural studies of lithiated enaminones: the 1-oxa-5-azapentadienyllithium fluxional heterocubane [(Pr^{i}NCMeCHCMeOLi)$_4$] and its dimeric hexamethylphosphoric triamide complex [{Pr^{i}NCMeCHCMeOLi·OP(NMe$_2$)$_3$}$_2$]. *J. Chem. Soc. Dalton Trans.* **1997**, *19*, 3421–3425. [CrossRef]
13. Olejník, R.; Padělková, Z.; Horáček, M.; Růžiča, A. Structure of β-diketiminates and β-aminoketones made from anisidines or chloroanilines: tin and lithium complexes. *Main Group Met. Chem.* **2012**, *35*, 13–27. [CrossRef]
14. Liu, Z.; Chen, H.-X.; Huang, D.; Zhang, Y.; Yao, Y.-M. A facile route to lithium complexes supported by β-ketoiminate ligands and their reactivity. *J. Organomet. Chem.* **2014**, *749*, 7–12. [CrossRef]
15. Clegg, W.; Dale, S.H.; Graham, D.V.; Harrington, R.W.; Hevia, E.; Hogg, L.M.; Kennedy, A.R.; Mulvey, R.E. Structural variations in bimetallic sodium–magnesium and sodium–zinc ketimides, and a sodium–zinc alkide–alkoxide–amide: Connections to ring-stacking, ring-laddering, and inverse crown concepts. *Chem. Commun.* **2007**, *16*, 1641–1643. [CrossRef] [PubMed]
16. Gregory, K.; Schleyer, P.v.R.; Snaith, R. Structures of organonitrogen–lithium compounds: Recent patterns and perspectives in organolithium chemistry. *Adv. Inorg. Chem.* **1991**, *37*, 47–142.
17. Mulvey, R.E. Meldola Medal Lecture. Ring-stacking and ring-laddering in organonitrogenlithium compounds: The development of concepts with wide applicability throughout lithium structural chemistry. *Chem. Soc. Rev.* **1991**, *20*, 167–209. [CrossRef]
18. Downward, A.; Chivers, T. Applications of the laddering principle—A two-stage approach to describe lithium heterocarboxylates. *Eur. J. Inorg. Chem.* **2001**, *9*, 2193–2201. [CrossRef]

19. Neculai, D.; Neculai, A.M.; Roesky, H.W.; Magul, J.; Bunkòczi, G. Synthesis and structure of a new fluorinated β-ketoiminato ligand and its lithium derivative. *J. Fluor. Chem.* **2002**, *118*, 131–134. [CrossRef]
20. Hsu, S.-H.; Li, C.-Y.; Chiu, Y.-W.; Chiu, M.-C.; Lien, Y.-L.; Kuo, P.-C.; Lee, H.M.; Huang, J.-H.; Cheng, C.-P. Synthesis and characterization of Cu(I) and Cu(II) complexes containing ketiminate ligands. *J. Organomet. Chem.* **2007**, *692*, 5421–5428. [CrossRef]
21. Lyashenko, G.; Saischek, G.; Judmaier, M.E.; Volpe, M.; Baumgartner, J.; Belaj, F.; Jancik, V.; Herbst-Irmer, R.; Mosch-Zanetti, N.C. Oxo-molybdenum and oxo-tungsten complexes of Schiff bases relevant to molybdoenzymes. *Dalton Trans.* **2009**, *29*, 5655–5665. [CrossRef] [PubMed]
22. Granum, D.M.; Riedel, P.J.; Crawford, J.A.; Mahle, T.K.; Wyss, C.M.; Begej, A.K.; Arulsamy, N.; Pierce, B.S.; Mehn, M.P. Synthesis and characterization of sterically encumbered β-ketoiminate complexes of iron(II) and zinc(II). *Dalton Trans.* **2011**, *40*, 5881–5890. [CrossRef] [PubMed]
23. Kakaliou, L.; Scanlon, W.J., IV; Qian, B.; Baek, S.W.; Smith, M.R., III; Motry, D.H. Five- and six-coordinate group 4 compounds stabilized by β-ketiminate and diketiminate ligands: Syntheses and comparisons between solid-state and solution structures. *Inorg. Chem.* **1999**, *38*, 5964–5977. [CrossRef] [PubMed]
24. Rat, C.; Comsa, C.; Silvestru, C. Dichlorido[(Z)-4-(2,6-diisopropylanilino)pent-3-en-2-one]dimethyltin(IV). *Acta Crystallogr. Sect. E Struct. Rep. Online* **2010**, *66*, m130. [CrossRef] [PubMed]
25. Comşa, C.; Cristea, A.; Varga, R.A.; Silvestru, C. Organotin(IV) complexes of β-ketimines. Crystal and molecular structure of OC(Me)CHC(Me)NHR-4 [R = $C_6H_3{}^iPr_{2\text{-}2}{}'$,6′; C_6H_4Me-4′], Bu_2SnCl_2(L) and [{Me_2SnCl}$_2$(L)]$_2$ [L = OC(Me)CHC(Me)NH($C_6H_3{}^iPr_{2\text{-}2}{}'$,6′)-4]. *Rev. Roum. Chim.* **2010**, *55*, 811–822.
26. Lugo, A.F.; Richards, A.F. Ketiminate-supported LiCl cages and group 13 complexes. *Eur. J. Inorg. Chem.* **2010**, *13*, 2025–2035. [CrossRef]
27. Lesikar, L.A.; Gushwa, A.F.; Richards, A.F. Synthesis, characterization, and steric hindrance comparisons of selected transition and main group metal β-ketoiminato complexes. *J. Organomet. Chem.* **2008**, *693*, 3245–3255. [CrossRef]
28. Lugo, A.F.; Richards, A.F. Ketiminato and ketimine Co, Eu, Cu and Fe complexes. *Inorg. Chim. Acta* **2010**, *363*, 2104–2112. [CrossRef]
29. Boeré, R.T.; Klassen, V.; Wolmershäuser, G. Synthesis of some very bulky *N*,*N*′-disubstituted amidines and initial studies of their coordination chemistry. *J. Chem. Soc. Dalton Trans.* **1998**, *24*, 2341–2345. [CrossRef]
30. Boeré, R.T.; Klassen, V.; Wolmershäuser, G. Superamidines 2. Synthesis of the bulky ligand *N*,*N*′-bis-(2,6-diisopropylphenyl)-trifluoroacetamidine and its molybdenum carbonyl complex. *Can. J. Chem.* **2000**, *78*, 583–589. [CrossRef]
31. Boeré, R.E.; Boeré, R.T.; Masuda, J.; Wolmershäuser, G. Preparation, X-ray structure, and dynamic solution behaviour of *N*,*N*′,*N*″-tris(2,6-diisopropylphenyl)-guanidine, and its reaction with molybdenum carbonyl. *Can. J. Chem.* **2000**, *78*, 1613–1619. [CrossRef]
32. Boeré, R.T.; Cole, M.L.; Junk, P.C.; Masuda, J.D.; Wolmershäuser, G. An *N*,*P*-disubstituted-2-aminophosphaalkene and lithium and potassium complexes of the deprotonated "phosphaamidinate" anion. *Chem. Commun.* **2004**, *22*, 2564–2565. [CrossRef] [PubMed]
33. Boeré, R.T.; Cole, M.L.; Junk, P.C. The syntheses and structures of some main group complexes of the sterically hindered *N*,*N*′-bis(2,6-diisopropylphenyl)-4-toluamidinate ligand. *New J. Chem.* **2005**, *29*, 128–134. [CrossRef]
34. Boeré, R.T.; Roemmele, T.L.; Suduweli Kondage, S.; Zhou, J.; Parvez, M. Five related *N*′-(2,2,2-trichloroethanimidoyl)benzene-1-carboximidamides. *Acta Cryst.* **2011**, *C67*, o273–o277.
35. Roemmele, T.L.; Boeré, R.T. 4-Methyl-*N*′-(2,2,2-trichloroethanimidoyl)benzene-1-carboximidamide. *Acta Cryst.* **2011**, *E67*, o3137. [CrossRef] [PubMed]
36. Vitanova, D.V.; Hampel, F.; Hultzsch, K.C. Rare earth metal complexes based on β-diketiminato and novel linked bis(β-diketiminato) ligands: Synthesis, structural characterization and catalytic application in epoxide/CO_2-copolymerization. *J. Organomet. Chem.* **2005**, *690*, 5182–5197. [CrossRef]
37. Boeré, R.T.; Gietz, T. Butylbis[μ-4-(2,4,6-trimethylphenylamino)pent-3-en-2-onato][4-(2,4,6-trimethylphenylamino)pent-3-en-2-on
Acta Cryst. **2009**, *E65*, m1137–m1138. [CrossRef] [PubMed]
38. Zhang, Z.-H.; Yin, L.; Wang, Y.-M. A general and efficient method for the preparation of β-enamino ketones and esters catalyzed by indium tribromide. *Adv. Synth. Catal.* **2006**, *348*, 184–190. [CrossRef]
39. Dudek, G.O.; Holm, R.H. Nuclear magnetic resonance studies of keto-enol equilibria. III. α,β-unsaturated-β-ketoamines. *J. Am. Chem. Soc.* **1962**, *84*, 2691–2696. [CrossRef]

40. Benito-Garagorri, D.; Kirchner, K.; Mereiter, K. *CCDC 274968: Experimental Crystal Structure Determination*; Cambridge Crystallographic Data Centre: Cambridge, UK, 2006. [CrossRef]
41. Wright, J.A. *CCDC 661234: Experimental Crystal Structure Determination*; Cambridge Crystallographic Data Centre: Cambridge, UK, 2008. [CrossRef]
42. Lin, T.-H.; Das, K.; Datta, A.; Leu, W.-J.; Hsiao, H.-C.; Lin, C.-H.; Guh, J.-H.; Huang, J.-H. Synthesis and characterization of ruthenium compounds incorporating keto-amine ligands. The applications of catalytic transfer hydrogenation and cancer cell inhibition. *J. Organomet. Chem.* **2016**, *807*, 22–28. [CrossRef]
43. Boeré, R.T.; Zhang, Y. Extremely bulky triarylphosphines incorporating 2,6-diisopropylphenyl substituents; consideration of steric shielding and steric pressure. *J. Organomet. Chem.* **2005**, *690*, 2651–2657. [CrossRef]
44. Zhang, L.; Brookhart, M.; White, P.S. Synthesis, characterization, and ethylene polymerization activities of neutral nickel(II) complexes derived from anilino-substituted enone ligands bearing trifluoromethyl and trifluoroacetyl substituents. *Organometallics* **2006**, *25*, 1868–1874. [CrossRef]
45. Kascheres, C.; Negri, G.; Gambardella, M.T.P.; Santos, R.H.A. X-ray crystal structure and AM1 optimized sctructure for 4-methylamino-3-diphenylacetyl-3-penten-2-one. *J. Braz. Chem. Soc.* **1994**, *5*, 31–37. [CrossRef]
46. Kabak, M.; Elmali, A.; Elerman, Y. Tautomeric properties, conformations and structure of *N*-(2-hydroxyphenyl)-4-amino-3-penten-2-on. *J. Mol. Struct.* **1998**, *470*, 295–300. [CrossRef]
47. Lide, D.R. *Handbook of Chemistry and Physics*, 85th ed.; CRC Press: Boca Raton, FL, USA, 2004.
48. Raissi, H.; Bakavol, M.; Jimenez-Fabian, I.; Tajabadi, J.; Mdoshfeghi, E.; Jalbout, A.F. Effect of substitution on the intramolecular hydrogen bonding of 4-amino-3-penten-2-one: Ab initio, AIM and NBO studies. *J. Mol. Struct. THEOCHEM* **2007**, *847*, 47–51. [CrossRef]
49. *APEX2, SAINT-Plus and SADABS*; Bruker AXS Inc.: Madison, WI, USA.
50. Sheldrick, G.M. A short history of *SHELX*. *Acta Cryst.* **2008**, *A64*, 112–122. [CrossRef] [PubMed]
51. Müller, P. (Ed.) *Crystal Structure Refinement: A Crystallographer's Guide to SHELXL*; OUP: Oxford, UK, 2006.
52. Spek, A.L. PLATON—A multipurpose crystallographic tool. *Acta Cryst.* **1990**, *A46*, C34.
53. Frisch, M.J.; Trucks, G.W.; Schlegel, H.; Scuseria, G.E.; Robb, M.A.; Cheeseman, J.R.; Montgomery, J.A., Jr.; Vreven, T.; Kudin, K.N; Burant, J.C.; et al. *Gaussian 03, Revision C.02*; Gaussian, Inc.: Wallingford, CT, USA, 2004.